Scripta Materialia 173 (2019) 66–69

Contents lists available at ScienceDirect

Scripta Materialia

journal homepage: www.elsevier.com/locate/scriptamat

In situ transmission electron microscopy investigation of continuous precipitation of Ni_3Mo in a superalloy formed by direct current magnetron sputtering

Megan G. Emigh, Jessica A. Krogstad *

Department of Materials Science and Engineering, University of Illinois at Urbana-Champaign, 1304 W Green St, Urbana, IL 61801, USA
Materials Research Laboratory, University of Illinois at Urbana-Champaign, 104 S Goodwin Ave, Urbana, IL 61801, USA

ARTICLE INFO

Article history:
Received 12 June 2019
Received in revised form 19 July 2019
Accepted 21 July 2019
Available online 9 August 2019

Keywords:
Precipitation
Transmission electron microscopy
Nickel alloys
Lattice defects
Phase transformation kinetics

ABSTRACT

In situ heating experiments explore a correlation between hexagonal close-packed (HCP) domains in sputter-deposited Ni-25Mo-8Cr films and the precipitation of HCP-type structures (Ni_3Mo). Dynamic observation of phase evolution in diffraction mode confirms that precipitation behavior in these defect-dense thin films is not merely kinetically accelerated; instead, the pathway is fundamentally altered. Short-range ordering (SRO) behavior was observed upon reaching 650 °C. SRO has been documented as part of the face-centered cubic (FCC)-precipitation pathway, but has not previously been reported for HCP-based precipitates. This effort provides evidence for continuous ordering of HCP-based precipitates from SRO domains in a mixed FCC-HCP metallic material.

Recent investigations of precipitation behavior in Ni-based superalloys formed by direct current magnetron sputtering have revealed dramatic departures from the precipitation behavior documented in conventionally cast alloys of the same composition [1,2]. The Ni-Mo-Cr alloy HAYNES® 242™, when processed *via* established routes, is a precipitation strengthened alloy, wherein a metastable $Ni_2(Mo,Cr)$ precipitate phase is the principle strengthening agent. However, when deposited as a sputtered film and subjected to a similar aging treatment, the DO_a variant of Ni_3Mo—which has a characteristic HCP-based packing structure—precipitates instead. This sputtered superalloy did not exhibit any measureable presence of the normally-expected, metastable $Ni_2(Mo,Cr)$ precipitate phase [2]. These observations suggested that the initial defect structure in the sputtered films can significantly alter either the precipitation kinetics, or the precipitation pathway, or both. Here, a series of *in situ* transmission electron microscope (TEM) heating experiments aim to distinguish between these possibilities.

Superalloys with a composition that favors a DO_a-type Ni_3Mo structure as a ground-state typically must pass through a series of complicated phase transformations in order to realize this equilibrium structure. The significant nucleation barrier for this HCP-based superstructure in an otherwise FCC matrix means that the intermediate, metastable $Ni_2(Mo,Cr)$ phase is typically present even after thousands of hours at elevated temperatures [3,4]. The apparent longevity of this metastable phase is often attributed to a combination of the following: the stabilizing nature of chromium in the $Ni_2(Mo,Cr)$ superstructure [5], and the multistep ordering process necessary to precipitate HCP-based DO_a (Ni_3Mo).

This multistep ordering/precipitation process within Ni—Mo alloys is known to be complex and may follow several possible variants depending on the specific alloying elements, their ratios, and the aging temperature. For the specific composition of Ni-25Mo-8Cr wt% in Haynes 242™, pre-service aging gives rise to short range ordering (SRO), followed by precipitation of the $Ni_2(Mo,Cr)$ structure. This metastable phase is resilient against further transformation and persists for the lifetime of a component under typical service conditions. However, given sufficient time at elevated temperature (or time and temperature following severe plastic deformation), the microstructure becomes overaged, and the metastable phase decomposes. Decomposition of the metastable phase introduces a sufficient population of geometrically necessary stacking faults in the superalloy, which give rise to local HCP-like ordering, thereby facilitating precipitation of the final, stable DO_a phase [6,7]. For clarity, Table 1 summarizes the expected long-term precipitation and ordering behavior in Haynes 242™. Specific temperatures and durations for the "extended" aging regime are omitted due to either significant disagreement in the existing literature on these precise values or very limited experimental observations.

Despite the complex precipitation behavior observed in Haynes 242™, distinguishing between the resulting superstructures by selected

* Corresponding author at: Department of Materials Science and Engineering, University of Illinois at Urbana-Champaign, 1304 W Green St, Urbana, IL 61801, USA.
E-mail address: jakrogst@illinois.edu (J.A. Krogstad).

https://doi.org/10.1016/j.scriptamat.2019.07.028
1359-6462/

Table 1
Expected aging behavior in an alloy with metastable $Ni_2(Mo,Cr)$ and fully stable DO_a-type Ni_3Mo. Intermediary steps based on behavior observed in similar alloys [6,7].

Heat treatment	Expected phase
As formed	Disordered FCC
Annealed (>1000 °C) and quenched	Development of short-ranged order
Mild aging treatment (~650 °C, 24–72 h)	Precipitation of $Ni_2(Mo,Cr)$
Extended aging	Decomposition of $Ni_2(Mo,Cr)$; FCC to HCP shear transformation; Stabilization of Ni_3Mo precipitates

area electron diffraction (SAED) is generally straightforward. In SAED, SRO is identified by diffuse superlattice reflections at every 1/4 and 3/4 $\{420\}_{FCC}$ fundamental reflection position, with an absence of intensity at $1/2\langle420\rangle_{FCC}$. The long range ordered (LRO) $Ni_2(Mo,Cr)$ can be identified by superlattice reflections at $1/3\ \langle220\rangle_{FCC}$ or $1/3\ \langle420\rangle_{FCC}$ fundamental reflection positions, and DO_a-type Ni_3Mo by superlattice reflections at *every* $1/4\ \langle420\rangle_{FCC}$ fundamental reflection position. These superstructure reflections arise from site-specific segregation of molybdenum during aging of the superalloy. Expected reflection positions are shown for clarity on the $[\bar{1}\bar{1}2]_{FCC}//[\bar{1}010]_{HCP}$ and $[111]_{FCC}//[0001]_{HCP}$ zone axes in Fig. 1 [8–10].

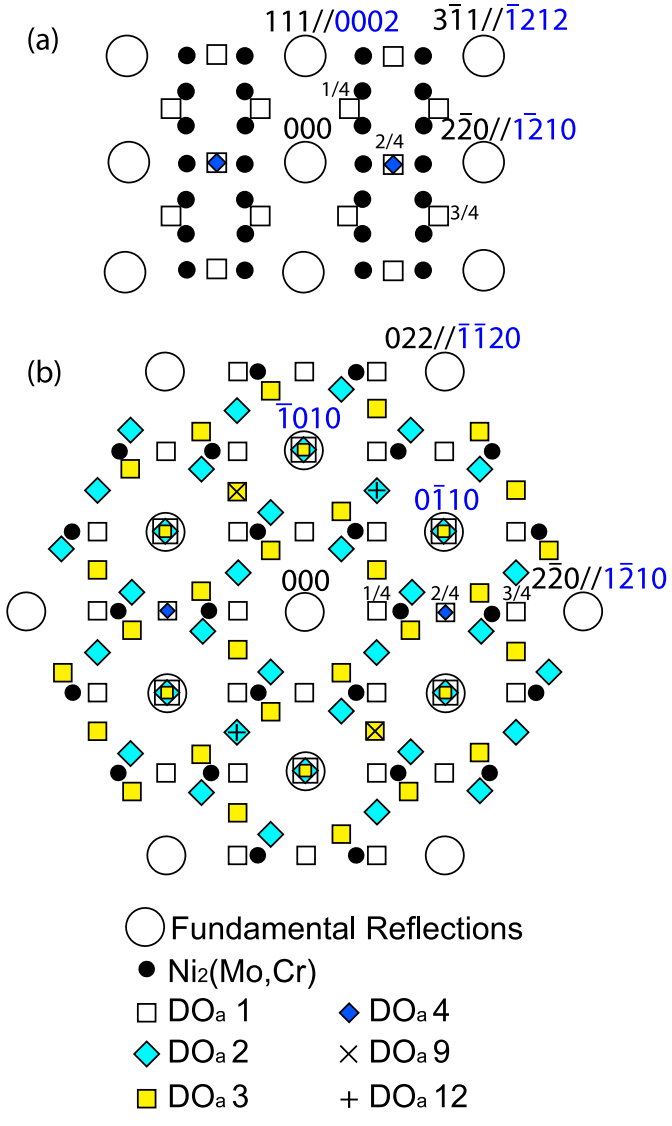

Fig. 1. Positions of select reflections of interest on the a) $[\bar{1}\bar{1}2]_{FCC}//[\bar{1}010]_{HCP}$ and b) $[111]_{FCC}//[0001]_{HCP}$ zone axes. Fundamental reflections are indicated by large, open circles; DO_a-type Ni_3Mo indicated by squares at every 1/4 fundamental position; $Ni_2(Mo,Cr)$ indicated by small dark circles at 1/3 fundamental reflection position. It should be noted that only one orientation of the Ni_3Mo structure is distinctly visible in the $[\bar{1}\bar{1}2]_{FCC}//[\bar{1}010]_{HCP}$ zone axis, but six may be visible in the $[111]_{FCC}//[0001]_{HCP}$ zone axis [8–10].

In the investigation preceding the *in situ* work presented here, corroborating evidence collected *via* high resolution scanning transmission electron microscopy (HRSTEM), x-ray diffraction (XRD), and conventional TEM indicated that these multistep phase transformations were entirely bypassed [2]. Instead, the fully-stable HCP-based DO_a phase precipitated continuously in sputtered Haynes 242™, circumventing the metastable $Ni_2(Mo,Cr)$ precipitate phase. The evident direct transformation of DO_a-type Ni_3Mo was rationalized as being facilitated by the high volume fraction of HCP-type domains in the as-deposited sputtered film. This present investigation attempts to further elucidate the early ordering behavior during aging of sputter deposited Haynes 242™. Additionally, this study explores whether precipitation of DO_a-Ni_3Mo was preceded by any sort of short range ordering.

For this investigation, single-target direct current magnetron sputtering (DCMS) was used to deposit Haynes® 242™ onto a water cooled, brass substrate. The alloyed target was sputtered at a constant power of 2400 W for 135 min, resulting in a deposition rate of about 4.4 nm/s, and a final film thickness of 35.75 μm. Following deposition, the superalloy was delaminated from the substrate, resulting in a free-standing film.

The film was prepared for *in situ* investigations *via* two methods, depending on the desired film orientation. The use of different orientations was necessary for comprehensive analysis due to the highly textured grain orientation. For plan-view observation, the material was jet polished with twin jets of 15 vol% perchloric acid in 85 vol% ethanol. For observation through the side view of the thin film, electron transparent specimens were extracted using a focused ion beam (FIB) lift out technique. FIB liftout was performed in an FEI Helios Nanolab Dual Beam and specimens were welded to a molybdenum grid with platinum.

Observation was carried out in a Jeol 2010 LaB_6 transmission electron microscope at 200 keV. In order to observe the early ordering behavior *in situ*, specimens were loaded in a Gatan double-tilt, water-cooled heating stage. The stage was heated resistively at a rate of 10 °C/min until the specimen reached 650 °C. This temperature was maintained throughout the duration of the *in situ* observation, which ran continuously for up to 10 h.

As previously established by electron diffraction orientation maps captured in TEM and reconstructed using ASTAR nanoMEGAS, the as-deposited structure of DCMS Haynes 242™ exhibited strong $[111]_{FCC}//[0001]_{HCP}$ orientation out-of-plane [2]. Perpendicular to the growth direction, the material exhibited dense planar faulting, colloquially referred to as nanotwinning. HRSTEM imaging showed that these 'nanotwins' were only a few atomic layers apart and were coherent on $\{111\}_{FCC}//\{0001\}_{HCP}$ planes. XRD confirmed that this high density of planar faults manifested as distinct domains of hexagonal close-packed and face-centered cubic ordering. These FCC/HCP domains existed in ratio of approximately 1:1, as determined by Rietveld analysis of powder-XRD data. No superstructure reflections were detected in selected area electron diffraction (SAED) patterns of the as deposited material as shown in Fig. 2, which includes both side and plan views. The absence of superstructure reflections in the as-deposited films is consistent with a chemically homogenous, disordered solid solution.

The prepared as-deposited specimens were heated to 650 °C *in situ* and that temperature was maintained for the duration of the examination. SAED patterns were captured periodically throughout the experiment. Qualitative observation of the early ordering behavior of DCMS Haynes 242™ *via* SAED required significant enhancement of the collected diffraction patterns while preserving the overall fidelity of the pattern. This was achieved though inversion of the diffraction contrast as well as enhancing the contrast and brightness on an image-by-

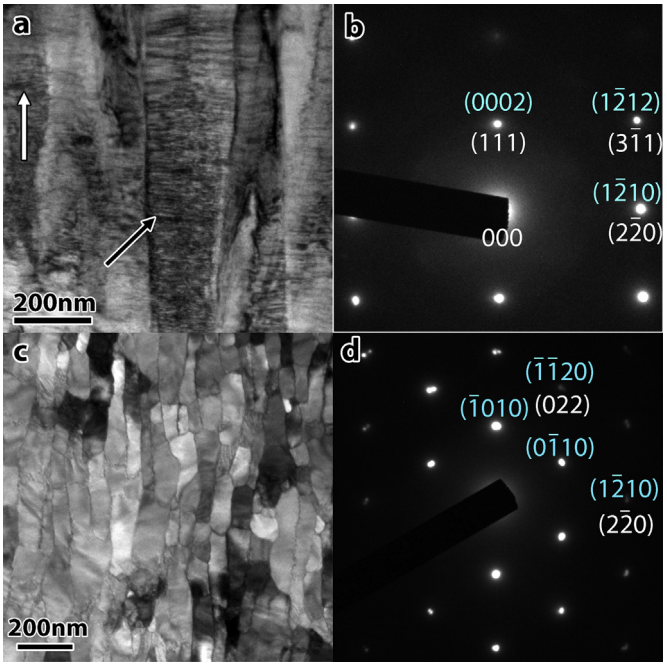

Fig. 2. a) Bright field image of the as-deposited material in the side view with growth direction indicated by white arrow, and nanotwinning indicated by black arrow; b) representative diffraction pattern from the $[\bar{1}\bar{1}2]_{FCC}//[\bar{1}010]_{HCP}$ orientation shows no superstructure reflections; c) bright field image of the as-deposited microstructure, shown in plan view, exhibits elongated grains and defect-rich grain boundaries; d) selected area electron diffraction pattern on the $[111]_{FCC}//[0001]_{HCP}$ zone axis shows both HCP (indexed in blue) and FCC (indexed in white) fundamental reflections.

image basis. This visual correction was necessary due to the intensity of the fundamental reflections, which prohibited the TEM camera and capture software (Digital Micrograph) from sufficiently correcting the contrast of the images *ab initio* for visual interpretation.

Fig. 3 shows the early ordering behavior in the side view of the material on the $[\bar{1}\bar{1}2]_{FCC}//[\bar{1}010]_{HCP}$ zone axis. Both as-captured patterns and the inverted, high-contrast images are presented here in order to preserve as-collected information, but also better present information on weak intensities. Shortly after reaching 650 °C, the specimens exhibited diffuse intensity at {1 1/2 0} intensity positions (these can also be thought of as the 1/4 and 3/4 $\langle 420\rangle_{FCC}$ fundamental positions as noted in Fig. 1), consistent with a short-range ordering phenomenon [11]. Additionally, reflections at 2/4 positions (which can also be considered the otherwise forbidden ⟨110⟩ reflection positions) were present, but were very diffuse and elongated. Intensity at the 2/4 positions is not associated with SRO, rather with the DO_a phase, which is characterized by reflections at *every* 1/4 $\langle 420\rangle_{FCC}$ fundamental position, *cf* Fig. 1. Over only 2.5 h of *in situ* heat treatment at 650 °C, the 2/4 position fundamental reflections sharpened while the already sharp intensities at 1/4 and 3/4 positions persisted, consistent with transformation to the DO_a-type Ni_3Mo phase. No intensity was observed at 1/3 $\langle 220\rangle_{FCC}$ or 1/3 $\langle 420\rangle_{FCC}$ fundamental reflection positions. The same ordering behavior was observed in plan view on the $[111]_{FCC}/[0001]_{HCP}$ zone axes, shown in Fig. 4. However, in plan view, six possible variants of the DO_a-structure can be observed. Not all of these are immediately apparent; however, over the duration of several hours at 650 °C, reflections from all six variants can be detected in this specific area of the foil. Given the thickness of the TEM lamellae and the stochastic probability of all DO_a-variants occurring in the sampling area, observation of all six variants may not be possible in all areas of the specimen. This may also contribute to the fact that positions of overlapping variant reflections did not fully sharpen over the course of 8 h; rather, these remain smeared, possibly indicating some degree of domain frustration.

Evidence of short-range ordering prior to precipitation of the DO_a-type Ni_3Mo merits further investigation. In conventionally processed alloys of this class, SRO is attributed to post-anneal quenching. Many authors, *e.g.* [3,6] or [11], have suggested a mechanism of continuous ordering of these SROs into the LRO $Ni_2(Mo,Cr)$ metastable phase. However, because SRO had not been observed in the as-deposited films, it had previously been posited that the DO_a-type Ni_3Mo precipitated *via* direct transformation, rather than a similar continuous ordering mechanism [2]. The cumulative *in situ* evidence presented here indicates that it was DO_a, not $Ni_2(Mo,Cr)$, that precipitated as a result of SRO. SRO reflections began to appear as soon as the heating stage began to approach the nominal aging temperature of 650 °C, and superstructure reflections associated with the DO_a-type superstructure coalesced continuously in relation to the SRO reflections.

Continuous transformation of a DO_a-type phase from SRO has not previously been reported in this class of alloys; however, given the mixed FCC/HCP closed-packed structure of the as deposited films, it is not difficult to rationalize. The difference between HCP-SRO and FCC-SRO may be likened to the small difference between the DO_a and DO_{22} superstructures. Both LRO superstructures are characterized by site-specific ordering of a substitutional atom (typically Al, Nb, or Mo) to

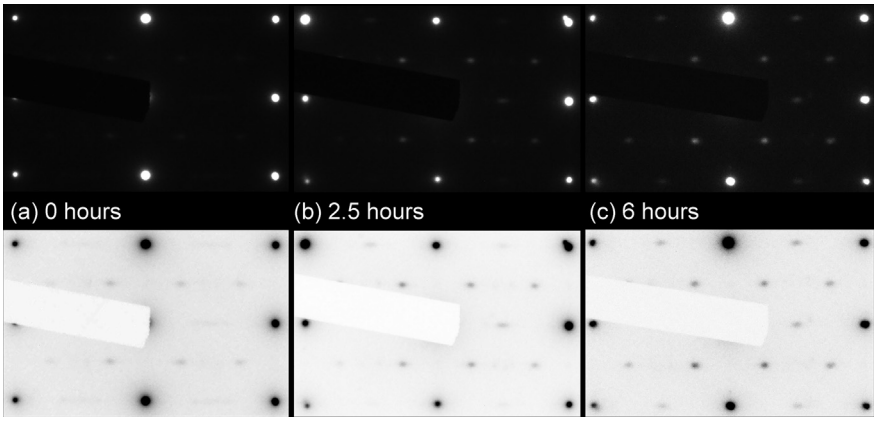

Fig. 3. Phase transformation through the side view of grains on the $[\bar{1}\bar{1}2]_{FCC}//[\bar{1}010]_{HCP}$ zone axis that exhibit exclusively Ni_3Mo precipitation (a) After only a few minutes at 650 °C, the side-view specimen already exhibited diffuse intensity at 1/4 and 3/4 fundamental lattice positions; furthermore, there is elongated intensity at 2/4 positions. b) After 2.5 h *in situ*, the specimens exhibited reflections at 1/4, 2/4, and 3/4 positions, consistent with the DO_a-Ni_3Mo superstructure. (c) After 6 h at 650 °C *in situ*, reflections associated with the stable DO_a-type Ni_3Mo phase remained, with slightly sharper intensities at 2/4 positions indicating more precise long range order. This is an expected behavior for a transition from short range ordering to long range ordering [8,14,15]. Inverted contrast of the diffraction lends clarity on reflection positions. Refer to Fig. 1(a) for complete indexing of this zone axis.

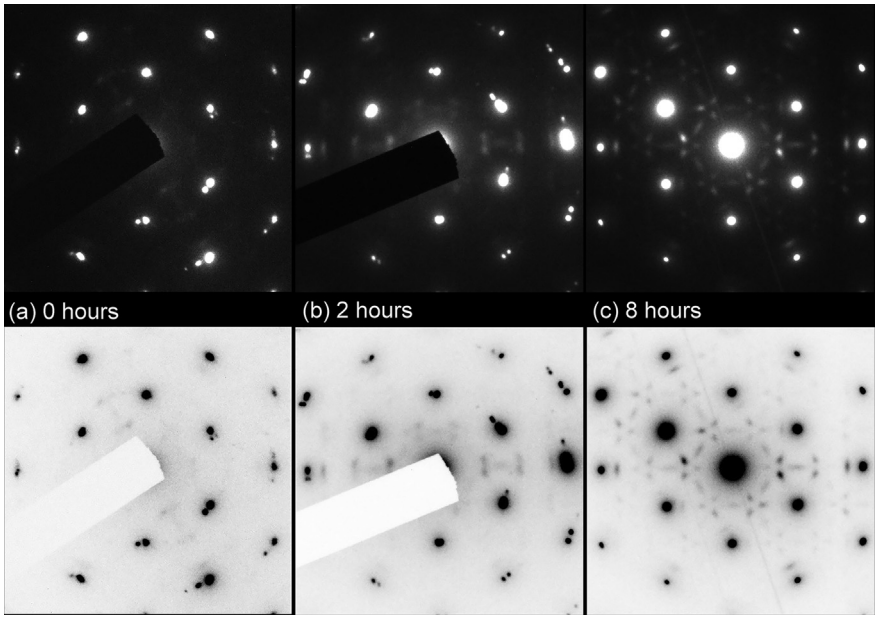

Fig. 4. Observation of the aging behavior through the plan view of the thin film, resulting in observation of the $[111]_{FCC}/[0001]_{HCP}$ orientation. a) After only a few minutes at 650 °C, sharp intensity at 1/4 and 3/4 fundamental reflection positions, associated with short range order, are visible. As with the $[\bar{1}\bar{1}2]_{FCC}//[\bar{1}010]_{HCP}$ orientation, elongated reflections are visible at 2/4 fundamental reflection positions. b) After approximately 2 h at 650 °C, the intensity of the superstructure reflections at 1/4, 2/4 and 3/4 fundamental reflection position has increased, indicating further ordering. c) After 8 h at 650 °C, the intensities at every 1/4 fundamental reflection position have sharpened even further, consistent with transformation to the DO_a-type Ni_3Mo structure. Inverted contrast of the diffraction lends clarity on reflection positions. Refer to Fig. 1(b) for complete indexing of this zone axis.

every fourth atomic plane. However, these structures differ by a stacking fault on the base $\{111\}_{FCC}//\{0001\}_{HCP}$ planes. This difference results in DO_{22} being an FCC-based precipitate, but DO_a being an HCP-based precipitate [12,13]. In a similar way, the SRO in this mixed close-packed material may be rationalized as partial segregation of the substitutional atoms in combination with a high density of $\{111\}_{FCC}//\{0001\}_{HCP}$ stacking faults as well.

Absence of the FCC-type metastable phase prior to transformation to the HCP-type stable DO_a phase was a consequence of pre-existing HCP-type domains that formed during the DCMS process. These HCP-like domains eliminated the need to form geometrically necessary planar defects, since the lattice upon which DO_a coherently precipitates was already present. This conclusion was previously presented in [2]; however, *in situ* observation of the transformation has confirmed the absence of any short-lived FCC-type precipitation that may have supported a case for accelerated phase evolution along the conventional pathway.

Transformation to the fully stable HCP-based DO_a-type phase is normally complex at temperatures below 800 °C, requiring spinodal decomposition of prior metastable phases and formation of a stacking fault [6,7]. Yet, when evolved from a nanotwinned DCMS thin film, transformation of the DO_a phase was both straightforward and rapid due to preexisting stacking faults in the as-deposited microstructure. In diffraction, continuous precipitation of DO_a was evident by sharp ⟨1 1/2 0⟩ SRO reflections in addition to elongated intensities at 2/4 ⟨420⟩ fundamental reflection positions. The elongation of these initial superlattice reflections was attributed to incomplete segregation of the solute Mo and Cr atoms to every fourth atomic plane. Over time, the elongated reflections sharpened into distinct, slightly diffuse reflections at 2/4 positions. This, in addition to the already-present superstructure reflections at 1/4 and 3/4 fundamental reflection positions, indicated substantial ordering to the DO_a-type Ni_3Mo phase, consistent with previous *ex situ* results and similar continuous ordering behavior reported previously [8,14,15]. The *in situ* observations presented here confirm an alternate phase evolution pathway for sputter deposited thin films of Haynes 242™ arising from the unique defect population introduced during the deposition process.

Thin films were deposited in the laboratory of T.P. Weihs at Johns Hopkins University. The authors would also like to acknowledge K.J. Hemker for many thoughtful discussions. Characterization was carried out in the Materials Research Laboratory Central Research Facilities, University of Illinois, Urbana-Champaign. This project was supported by the Department of Materials Science and Engineering at the University of Illinois at Urbana-Champaign and by NSF CMMI Award #1761189.

References

[1] D.E. Burns, Y. Zhang, T.P. Weihs, K.J. Hemker, Thin Solid Films 558 (2014) 20–23, https://doi.org/10.1016/j.tsf.2014.02.051.
[2] M.G. Emigh, R.D. McAuliffe, C. Chen, J.C. Mabon, T. Weihs, K.J. Hemker, D.P. Shoemaker, J.A. Krogstad, Acta Mater. (2018)https://doi.org/10.1016/J.ACTAMAT.2018.07.007.
[3] M. Kumar, V.K. Vasudevan, D. Harker, B. Chakravarti, E.A. Starke, B.G. Lefevre, T. Saburi, H. Fujii, S. Nenno, C.R. Brooks, J.E. Spruiell, E.E. Stansbury, K. Vasudevan, E. E. Stansbury, D. De Fontaine, S. Banerjee, K. Urban, M. Wilkens, MRS Proc. 213 (1990) 187, https://doi.org/10.1557/PROC-213-187.
[4] S. Dymek, M. Wróbel, M. Dollar, Scr. Mater. 43 (2000) 343–348, https://doi.org/10.1016/S1359-6462(00)00420-6.
[5] M. Sundararaman, L. Kumar, G.E. Prasad, P. Mukhopadhyay, S. Banerjee, Metall. Mater. Trans. A 30 (1999) 41–52, https://doi.org/10.1007/s11661-999-0194-6.
[6] D. Schryvers, G. Van Tendeloo, S. Amelinckx, Phys. Status Solidi 87 (1985) 401–415, https://doi.org/10.1002/pssa.2210870202.
[7] G. Van Tendeloo, R. De Ridder, S. Amelinckx, Phys. Status Solidi 27 (1975) 457–468, https://doi.org/10.1002/pssa.2210270215.
[8] M. Kumar, V.K. Vasudevan, Acta Mater. 44 (1996) 1591–1600, https://doi.org/10.1016/1359-6454(95)00258-8.
[9] S. Mahadevan, S. Nalawade, J.B. Singh, A. Verma, 7th Int. Symp. Superalloy 718 Deriv. TMS, 2010https://doi.org/10.1002/9781118495223.ch57.
[10] W.E. Quist, R. Taggart, D.H. Polonis, Metall. Trans. A. 2 (1971) 825–832, https://doi.org/10.1007/BF02662742.
[11] A. Verma, N. Wanderka, J.B. Singh, M. Sundararaman, J. Banhart, J. Alloys Compd. 586 (2014) 561–566, https://doi.org/10.1016/j.jallcom.2013.10.086.
[12] A. Arya, S. Banerjee, G.P. Das, I. Dasgupta, T. Saha-Dasgupta, A. Mookerjee, Acta Mater. 49 (2001) 3575e3587, https://doi.org/10.1016/S1359-6454(01)00235- X.
[13] M. Sundararaman, P. Mukhopadhyay, S. Banerjee, Metall. Trans. A. 19 (1988) 453–465, https://doi.org/10.1007/BF02649259.
[14] S. Banerjee, K. Urban, M. Wilkens, Acta Metall. 32 (1984) 299–311, https://doi.org/10.1016/0001-6160(84)90103-2.
[15] D. De Fontaine, Acta Metall. 23 (1975) 553–571, https://doi.org/10.1016/0001-6160(75)90096-6.